land

Article

Spatiotemporal Dynamics of Land Cover and Their Driving Forces in the Yellow River Basin since 1990

Shirui Zhao [1,2], Zemeng Fan [1,2,3,*] and Xing Gao [1,2]

[1] State Key Laboratory of Resources and Environment Information System, Institute of Geographical Sciences and Natural Resources Research, Chinese Academy of Sciences, Beijing 100101, China
[2] College of Resources and Environment, University of Chinese Academy of Sciences, Beijing 100049, China
[3] Jiangsu Center for Collaborative Innovation in Geographical Information Resource Development and Application, Nanjing 210023, China
* Correspondence: fanzm@lreis.ac.cn

Abstract: The national strategy for ecological protection and high-quality development is raising the ecological security protection to an unprecedented level in the Yellow River Basin (YRB) of China. Due to the explicitly analyzed land cover changes under climate change and rapid urbanization in the YRB area since 1990, land cover dynamic degree index, transfer matrix, and geo-detector method were used to explicate land cover changes and their key driving factors, based on the spatial data of land cover from 1990 to 2020. The results show that grasslands, croplands, and forests are the main land cover types, accounting for 48.37%, 25.05%, and 13.50%, respectively, of the total area in the YRB area. Grassland, cropland, and cropland are the major land cover type, accounting for 61.49%, 37.13%, and 66.33%, respectively, in the upstream, midstream, and downstream of the YRB area. Built-up land has showed a continual increasing trend, and its dynamic degree was up to 3.38% between 2010 and 2020. Population density was a key factor for land cover change, with an average contribution rate of 0.264; then, elevation and temperature also expressed an important role to drive the land cover change in the YRB area during the period from 1990 to 2020.

Keywords: land cover; spatiotemporal dynamics; diving forces; Yellow River Basin

Citation: Zhao, S.; Fan, Z.; Gao, X. Spatiotemporal Dynamics of Land Cover and Their Driving Forces in the Yellow River Basin since 1990. *Land* **2022**, *11*, 1563. https://doi.org/10.3390/land11091563

Academic Editors: Wenze Yue, Yang Chen and Yang Zhang

Received: 12 August 2022
Accepted: 10 September 2022
Published: 14 September 2022

1. Introduction

Land is the foundation of human life and social development, as well as an indispensable resource for human activities. Land cover change is an important indicator that characterizes the impacts of human activities on the natural ecosystems [1]. In recent years, land cover change is also a hot issue in global climate change research. In 2005, the Global Land Project (GLP), in collaboration with the international geosphere and biosphere program (IGBP) and human factors of the Global Change Program (IHDP), a key step in resolving the mutually beneficial relationship between man and land [2]. Under the joint promotion of IGBP and IHDP, the research on land cover has become one of the research cores of global environmental change [3–5]. Land cover change has an obvious impact on river runoff, biological abundance, and soil erosion. If the land cover is unreasonable, it may cause adverse effects on the ecological environment security of the Yellow River Basin (YRB) of the China area. The analysis of land cover change and its driving forces can provide a scientific basis for rational allocation of water and land resources.

The Yellow River, the mother river of China, has a very special status, and has been nourishing the residents lived in the Yellow River Basin (YRB) of China for thousands of years. At present, there are 107 million peoples lived in the YRB area, where the area of cropland is 13 million km^2. YRB crosses the arid, semi-arid, and semi-humid areas of China. YRB is an important ecological barrier in northern China, including the Qinghai-Tibet Plateau, Loess Plateau, and North China Plain [6]. The western part of YRB is located in the frigid zone. The northwest part is adjacent to the Gobi desert, the northern part has a large area of desert, and the central part is an area with serious soil erosion; the ecological environment is fragile. The midstream area and downstream area of YRB are one of the regions where the relationship between man and land is relatively tense. Along with the influence of climate change and human activities, the ecological environment question also further highlights in the YRB area [7].

At present, many scholars have studied land cover in different research areas with different emphases, related research combining land cover change has been extensively conducted, which included the process, pattern, land cover transition [8,9], dynamic driving forces, and eco-environmental effects of land cover change [10–12]. For example, Surya et al. analyzed the spatial interaction and sustainable development, in terms of land cover change in the Metropolitan Urban Areas, South Sulawesi Province, Indonesia [13]. Teklay et al. investigated the effects of accounting dynamic land cover on hydrological responses in Gummara watershed, Ethiopia [14]. Lambin et al. examined the relationship between land cover and socioeconomic economy [8]. Rimal et al. explicated the relationship among urbanization, land cover dynamics, and multiple disaster and risk analysis in the Pokhara Valley from 1990 to 2013 [9]. Dewan am et al. analyzed land cover dynamics in Dhaka, Bangladesh, based on the satellite imagery [15]. Kalnay E et al. described the impacts of climate change on land cover change [16]. Qingliu et al. evaluated and forecast the carbon storage of Hainan Island, based on land cover dynamics [17].

Moreover, there are also many efforts to analyze the driving factors of land cover change and have further supplemented the research on land cover change. The current analysis of the driving factors of land cover change mainly includes qualitative and quantitative analysis. Qualitative analysis methods cannot quantitatively express the impact of various drivers on land cover change [18,19], while quantitative methods can quantify the impact of various drivers on land cover change [20,21]. However, neither method can reflect the relationship between driving factors and land cover changes in spatial location [22]. GeoDetector is a statistical method that detects spatial differences to analyze their drivers [23,24]. The GeoDetector method can be used to analyze the spatial relationship between different driving factors of land cover change [25–28].

With the rapid population and economic growth, as well as climate change, land cover of YRB occurred a series of dramatic changes since 1990. Therefore, regarding how to explicitly analyze the spatiotemporal dynamics of land cover and clearly explicate the key driving forces of land cover in the YRB area since 1990, it is helpful to clearly understand the changes of vegetation cover and formulate relevant plans in a timely and effective manner to better protect the ecological environment in the YRB area. The paper is aimed to clearly explicate the spatiotemporal dynamics of land cover and their driving forces in the YRB area during the period from 1990 to 2020, based on the spatial data of land cover in 1990, 2000, 2010, and 2020.

2. Materials and Methods

2.1. Study Area

The YRB (96°–119°5′ E, 32°–42° N), located in the Bayan Har Mountains in Qinghai Province, flows through nine provinces and regions: Qinghai, Sichuan, Gansu, Ningxia, Inner Mongolia, Shaanxi, Shanxi, Henan, Shandong, and, finally, to Bohai Sea in Kenli County. The area of the Yellow River basin is 79.46×10^4 km^2. The YRB can generally be divided into three watersheds: the upstream area (UA), midstream area (MA), and downstream area (DA). The terrain of the YRB (Figure 1) declines step-by-step, from west to east, with a huge difference in height, and can be divided into three levels, which are roughly in the form of a ladder. The first staircase consists of a series of mountains, with an average elevation of more than 4000 m, including Bayan Har Mountains, Qilian Mountains, etc. The second staircase is located between 1000–2000 m, including Loess Plateau, Hetao Plain, Ordos Plateau, etc.; the elevation of third step is less 500 m, and the terrain is relatively gentle. There are significant differences among different regions in the YRB, with a semi-humid climate in the southeast, a semi-arid climate in the middle and arid climate in the northwest [29]. Climatic factors also vary greatly in different years, seasons, and months in the same region.

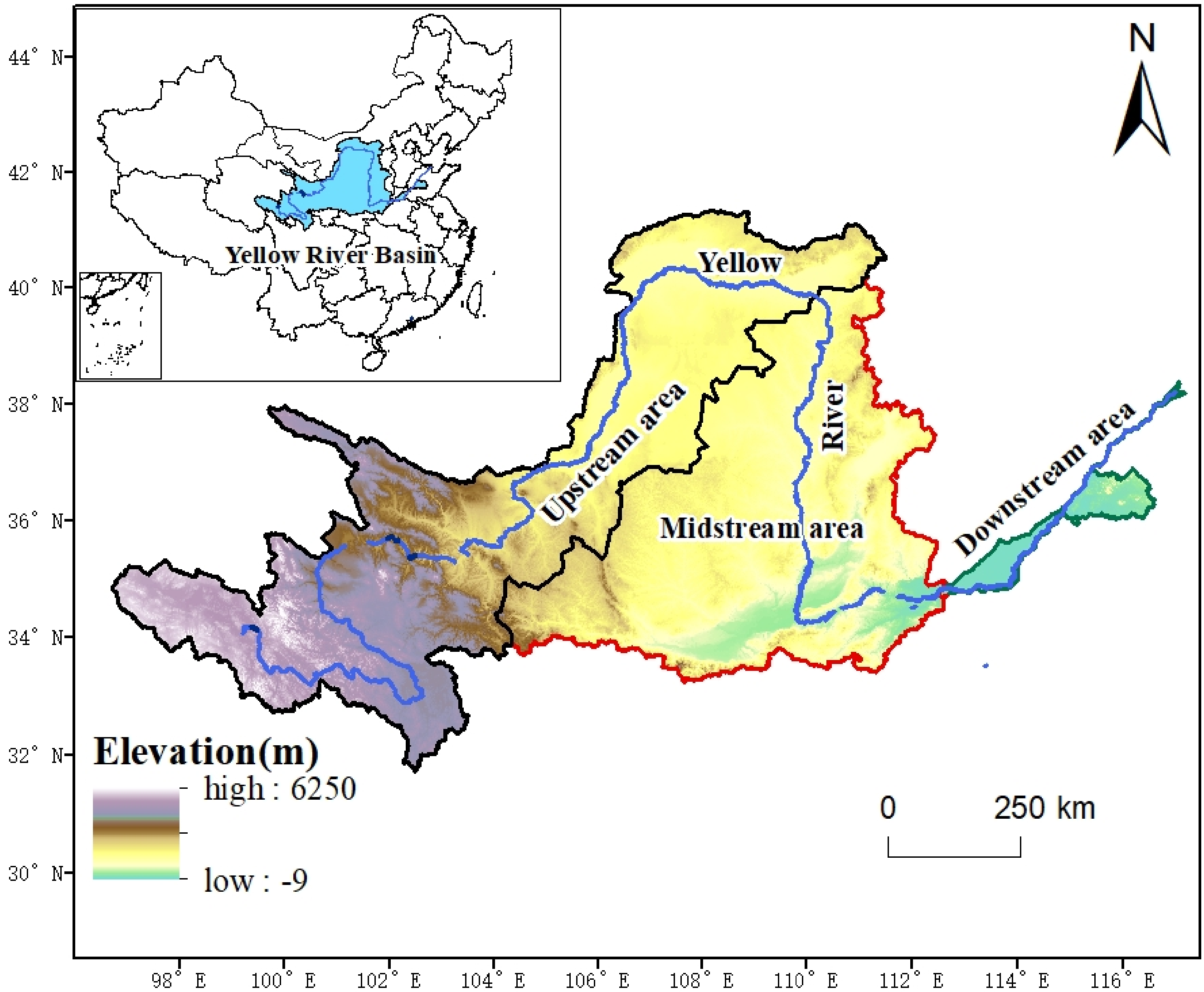

Figure 1. Spatial location and DEM of the Yellow River Basin (YRB).

There are many kinds of ecosystems in the YRB, which are beneficial to the distribution of various vegetation types. The vegetation cover of cropland, grassland, woodland, and shrub occupies 98% of the whole basin, and the areas of tundra, herbaceous swamp, and other vegetation types just cover 2%.

2.2. Data Sources

The land cover data adopted in this study in 1990, 2000, 2010, and 2020 were obtained from the Resource and Environmental Science Data Center of the Chinese Academy of Sciences (RESDC) (http://www.resdc.cn) (accessed on 1 March 2021) [30–32]. According to the current classification of land cover in China [33], the land cover types were divided into forest, grassland, cropland, built-up land, water area, built-up land, desert, or other land. The DEM data comes from (RESDC) (http://www.resdc.cn/), with a spatial resolution of 250 m × 250 m. The precipitation, temperature, population density, and GDP data of the YRB also come from RESDC (http://www.resdc.cn).

2.3. Methods

2.3.1. Dynamic Degree of Land Cover

The change ratio of land cover percentage can be used to reflect the proportion of the area of a certain land cover type in whole YRB area, which can be formulated as:

$$B = \frac{K_1}{K} \times 100\% \quad (1)$$

where K_1 is the area of a land cover type, and K represents the total area of the study area.

The dynamic degree index of land cover was used to compute the change rate of a certain type of land cover in a certain period of time [34], which can be formulated as:

$$\mathrm{R_d} = \frac{K_2 - K_1}{K_1} \times \frac{1}{\mathrm{t_2} - \mathrm{t_1}} \times 100\% \quad (2)$$

where $\mathrm{R_d}$ is the dynamic degree of a land cover type during the study period; K_1 and K_2, respectively, represent the area of the land cover type at the beginning period $\mathrm{t_1}$ and the end period $\mathrm{t_2}$.

2.3.2. The Transfer Matrix of Land Cover Change

The transfer matrix method was used to reflect the conversion between different land cover types and conversion area [35], which can be formulated as:

$$S_{ij} = \begin{Bmatrix} K_{11} & \cdots & K_{1n} \\ \vdots & \ddots & \vdots \\ K_{n1} & \cdots & K_{nn} \end{Bmatrix} \quad (3)$$

where S_{ij} represents the area of initial land cover type i converted to final land cover type j, and n represents the total number of land cover types; i, j (i, j = 1, 2, . . . , n) represent the types of land cover at the beginning and end of the study.

2.3.3. GeoDetector Method of Land Cover

GeoDetector is a statistical method [24] that could be used explicate the spatial differences among different driver factors of land cover change. Thus, the GeoDetector has been introduced to analyze the spatial relationship between different land cover types and different driving factors of land cover change.

Factor detector was used to identifies the driving factors of land cover responsible for the independent variable, which could be formulated as follows:

$$q = 1 - \frac{\sum_{h=1}^{L} N_h \sigma_h^2}{N\sigma^2} \quad (4)$$

where q reflects the degree of influence of driving factors on land cover, L is the number of driving factors, N_h and N are the units of sub-region h and the total study area, and σ_h^2 and σ^2 are the discrete variances of the land cover in the sub-region h and the land cover in the study area. The q value is between 0 and 1, and the large value of q indicates that the driving factor has a large influence on the land cover; on the contrary, the influence is small.

Moreover, the ecological detector was used to judge whether there is a significant difference in the impact of the two driving factors (X_1 and X_2) on the spatial pattern of land cover change, and uses the F statistic to test it:

$$F = \frac{N_{X_1}\left(N_{X_2} - 1\right) SSW_{X_1}}{N_{X_2}\left(N_{X_1} - 1\right) SSW_{X_2}} \quad (5)$$

$$SSW_{X_1} = \frac{\sum_{h=1}^{L_1} N_h {\sigma_h}^2}{N\sigma^2} \quad (6)$$

$$SSW_{X_2} = \frac{\sum_{h=1}^{L_2} N_h {\sigma_h}^2}{N\sigma^2} \tag{7}$$

where N_{X_1} and N_{X_2} represent the sample number of two factors (X_1 and X_2). SSW_{X_1} and SSW_{X_2} reflect the sum of variance of each class formed by two factors (X_1 and X_2). L_1, and L_2 represents the number of classes for variable X_1 and X_2. *F*-test was used to determine the significance level of *F* statistic.

3. Results

3.1. Spatial Distribution of Land Cover in YRB

The distribution pattern of land cover in YRB area clearly shows a spatial difference from the upstream area to downstream area (Figure 2). The forest is mainly distributed in the mountains and hilly areas of upstream and midstream areas of YRB, especially in Hengduan Mountains, Qilian Mountains, Qinling Mountains, and Ziwu mountains. The grassland of the YRB is mainly distributed in the plateau and highland areas in the YRB, such as the eastern part of Qinghai-Tibet Plateau, middle and north of Loess Plateau, and southwest of Inner Mongolia Plateau. Cropland is mainly located in the basin and plain area of YRB, such as the Weihe Basin and the North China Plain. Built-up land is mainly distributed in the urbans and their adjacent areas in the YRB. In addition to the Yellow River itself, the water area is mainly distributed in the headwater areas of the upstream area of YRB. Desert or other land is mainly distributed in the upstream area of the YRB and Inner Mongolia Plateau.

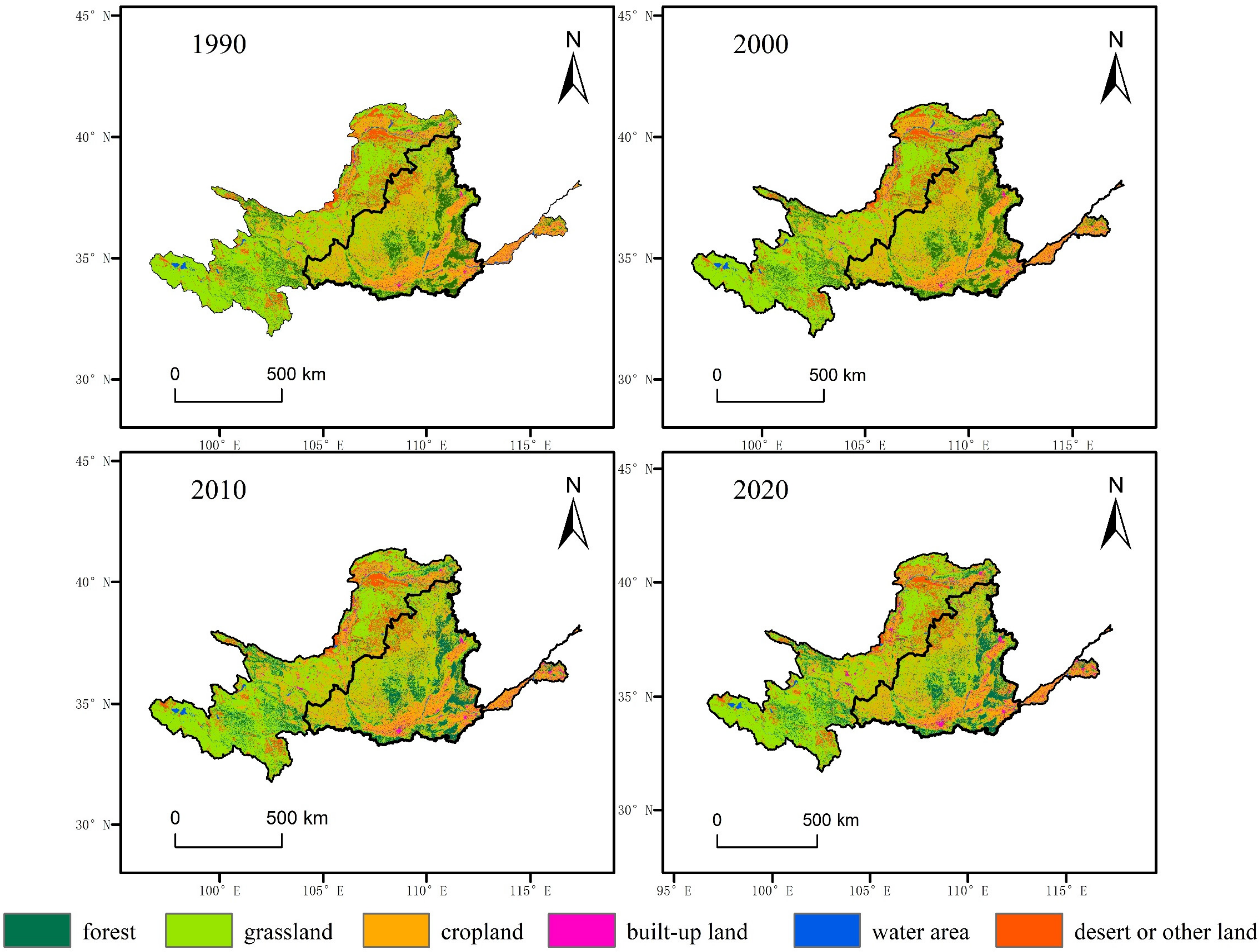

Figure 2. Spatial distribution of land cover in the YRB area during the period from 1990 to 2020.

The analyzed results (Table 1) show that the area of grassland was the largest, accounting for 48.62% of the total area of YRB between 1990 and 2020. The area of water area was the least, accounting for 1.77% of the total area of YRB. The terrain surface of YRB was dominated by the three land cover types of forest, grassland, and cropland, and the ratio of area was up to 85% of the total area of YRB. In the upstream area of YRB, the land cover was dominated by grassland, accounting for more than 60% of the whole upstream area, followed by cropland, desert, and other land. In the midstream area of YRB, cropland and grassland were the mainly land cover types, and the ratio of that is about 70% of the whole midstream area. In the downstream area of YRB, cropland is the mainly land cover type, and its ratio accounts for more than 65% of the downstream area.

Table 1. The areas of land cover in the YRB area during the period from 1990 to 2020.

Land-Cover Type		1990		2000		2010		2020	
		Area (km^2)	%	Area (km^2)	%	Area (km^2)	%	Area (km^2)	%
Forest	UA	35,585.47	8.35	35,476.46	8.32	36,633.54	8.59	36,770.55	8.63
	MA	67,144.65	19.45	66,937.64	19.39	69,209.8	20.05	68,983.78	19.98
	DA	1622.11	7	1633.11	7.04	1543.11	6.66	1541.11	6.65
	total	104,352.23	13.13	104,047.21	13.09	107,386.45	13.51	107,295.44	13.50
Grassland	UA	265,971.43	62.4	263,615.27	61.85	262,927.22	61.69	262,079.16	61.49
	MA	120,573.35	34.93	121,212.4	35.12	122,433.48	35.47	121,140.39	35.09
	DA	1616.11	6.97	1606.11	6.93	1164.08	5.02	1163.08	5.02
	total	388,160.89	48.85	386,433.78	48.63	386,524.78	48.64	384,382.63	48.37
Cropland	UA	56,409.91	13.23	58,533.06	13.73	56,010.88	13.14	55,509.85	13.02
	MA	136,354.45	39.5	136,544.46	39.56	130,865.07	37.91	128,183.88	37.13
	DA	15,685.09	67.65	15,961.11	68.84	15,663.09	67.56	15,380.07	66.33
	total	208,449.45	26.23	211,038.63	26.56	202,539.04	25.49	199,073.8	25.05
Built-up land	UA	6139.43	1.44	6510.45	1.53	7348.51	1.72	9848.68	2.31
	MA	8293.57	2.4	9204.64	2.67	10,423.72	3.02	14,813.03	4.29
	DA	2532.18	10.92	2714.19	11.71	3407.24	14.7	3670.25	15.83
	total	16,965.18	2.14	18,429.28	2.32	21,179.47	2.67	28,331.96	3.57
Water area	UA	8859.61	2.08	8912.62	2.09	8984.62	2.11	9233.64	2.17
	MA	3807.26	1.1	3643.25	1.06	3765.26	1.09	3736.26	1.08
	DA	1557.11	6.72	1181.08	5.09	1334.09	5.75	1361.09	5.87
	total	14,223.98	1.79	13,736.95	1.73	14,083.97	1.77	14,330.99	1.80
Desert or other land	UA	53,274.69	12.5	53,192.69	12.48	54,335.77	12.75	52,798.66	12.39
	MA	9010.62	2.61	7641.53	2.21	8486.59	2.46	8326.58	2.41
	DA	173.01	0.75	90.01	0.39	74.01	0.32	70	0.3
	total	62,458.32	7.86	60,924.23	7.67	62,896.37	7.92	61,195.24	7.70

3.2. Area Change of Land Cover in YRB

The analyzed results of land cover changes between 1990 and 2020 in the YRB area (Figure 2 and Table 1) show that cropland and grassland showed a continual decreasing trend, with average decreases of 3125.22 and 1259.42 km^2, respectively, per decade. Built-up land showed a continual increasing trend, with average increased by 3788.93 km^2 per decade. Forest and water area generally showed an increasing trend, with respectively average increased by 981.07 and 35.67 km^2, respectively, per decade. Desert or other land generally showed a decreasing trend, with average decreased by 421.03 km^2 per decade.

From the upstream, midstream, and downstream area of YRB perspectives, in the upstream area of YRB, built-up land had the largest increasing ratio, with average increased by 20.14% per decade between 1990 and 2020. Cropland had the largest decreasing ratio, with average decreased by 0.53% per decade.

In the midstream area of YRB, built-up land also had the largest increasing ratio, with average increased by 26.14% per decade between 1990 and 2020. Desert or other land had the largest decreasing ratio, with average decreased by 2.53% per decade.

In the downstream area of YRB, built-up land still had the largest increasing ratio, with average increased by 14.98% per decade between 1990 and 2020. Desert or other land had the largest decreasing ratio, with average decreased by 19.85% per decade.

3.3. Dynamic Degree of Land Cover Change in YRB

The calculated results of the dynamic degrees of each land cover type during the three periods from 1990 to 2000, 2000 to 2010, and 2010 to 2020 were listed as Table 2. From 1990 to 2020, the dynamic degrees of water area and grassland were the least number, respectively, at only 0.03% and −0.03% per year. The dynamic degree of forest and built-up land showed an increasing trend, especially that of built-up land is the highest growth rate (2.23% per year). The dynamic degree of cropland had the highest negative growth rate (−0.15% per year). The dynamic degree of forest was small (0.09% per year) between 1990 and 2010, with the biggest (0.32% per year) between 2000 and 2010. The dynamic degree of grassland and water area was stable than that of other land cover types during the periods from 1990 to 2020. The dynamic change of desert or other land between 1990 and 2010 was small (−0.07% per year), and that between 2000 and 2010 was the largest (0.32% per year). The dynamic degree built-up land was the largest (3.38% per year) between 2010 and 2020.

Table 2. Dynamics degree of land cover change in YRB from 1990 to 2020.

Land-Cover Type	Land Cover Dynamics Degree (%/Year)			
	1990–2000	2000–2010	2010–2020	1990–2020
Forest	−0.03	0.32	−0.01	0.09
Grassland	−0.04	0.00	−0.06	−0.03
Cropland	0.12	−0.40	−0.17	−0.15
Built-up land	0.86	1.49	3.38	2.23
Water area	−0.34	0.25	0.18	0.03
Desert or other land	−0.25	0.32	−0.27	−0.07

3.4. Transform Trend of Land Cover in YRB

In order to directly reflect the distribution patterns of land cover and the transform relationship between different land cover types, we calculated the transfer matrix of land cover and drew the transform charts of land cover type (Figure 3) from 1990 to 2000, 2000 to 2010, and 2010 to 2020. In the Figure 3, the arrows indicate the conversion direction of different land cover types, and the thickness arrows represent the transformed area of different land cover type. The analyzed results of transform between different land cover types show that the major change patterns of different land cove types were the mutual conversion between grassland and desert or other land, grassland and cropland, and that between cropland and built-up land.

Between 1990 and 2000 (Table 3), there was 1211.09 km^2 water area transferred to other land cover types, accounting for 8.51% of the area of water area in 1990. There was 3246.23 km^2 desert or other land transferred to other land cover types, accounting for 5.20% of the area of desert or other land in 1990. The transformed area of built-up land is less than that of other land cover types, which was only 5 km^2. Among them, 75.05% of the desert or other land type land was transformed to grassland, and 74.36% of the forest was converted to grasslands.

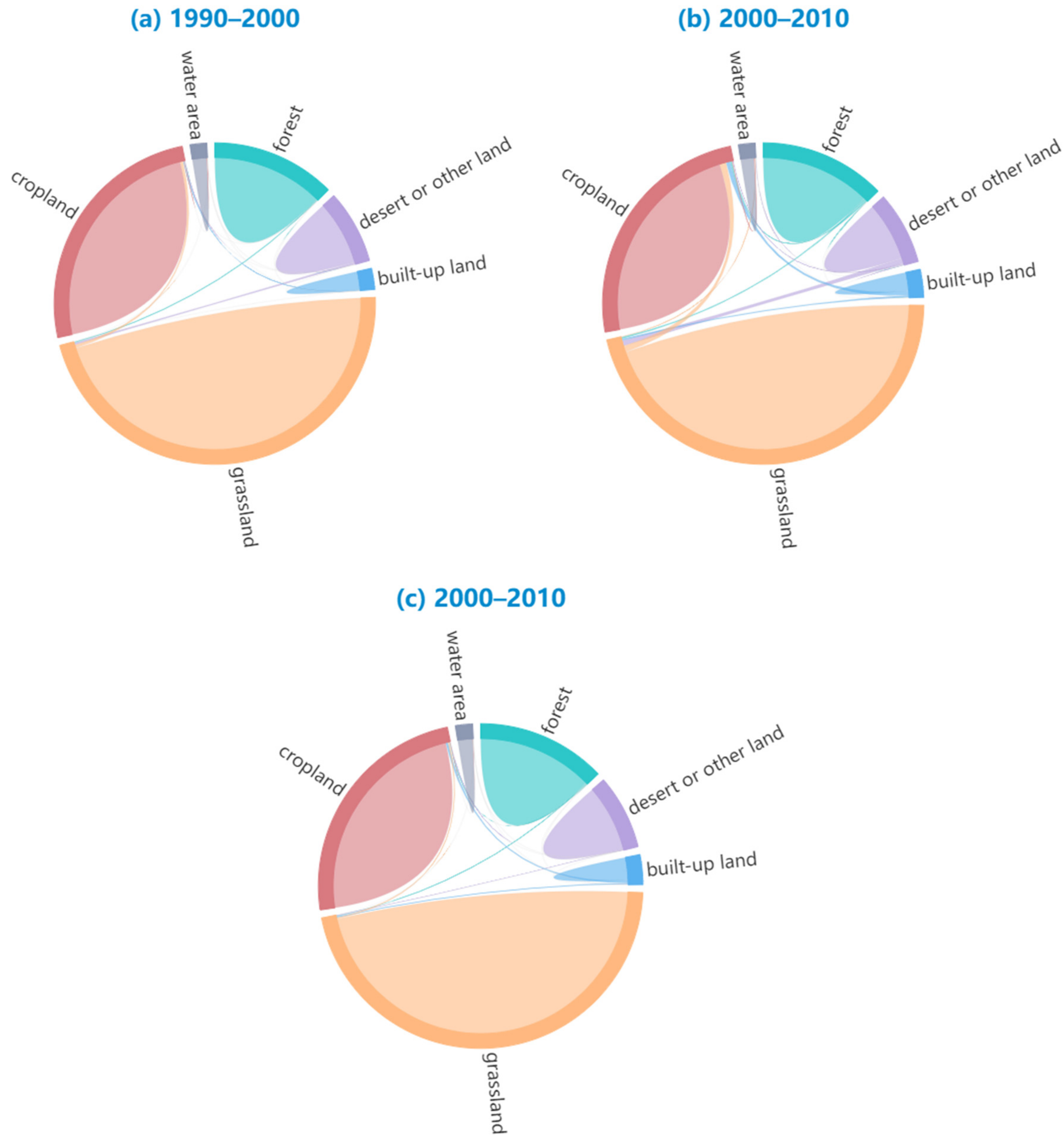

Figure 3. Land cover transfer matrix of YRB between 1990 and 2000 (**a**), 2000 and 2010 (**b**), and 2010 and 2020 (**c**).

Table 3. Transformed areas of each land cover type in YRB between 1990 and 2000 (unit: km^2).

1990 / 2000	Forest	Grassland	Cropland	Built-Up Land	Water Area	Desert or Other Land	2000 Total
Forest	102,819.12	845.06	264.02	0	25	94.01	104,047.2
Grassland	1140.08	381,205.41	1431.1	1	219.02	2436.17	386,432.8
Cropland	294.02	4366.3	204,950.2	1	848.06	578.04	211,037.6
Built-up land	39	158.01	1209.08	16,960.18	19	44	18,429.27
Water area	11	315.02	304.02	0	13,012.9	94.01	13,736.95
Desert or other land	49	1270.09	290.02	3	100.01	59,212.1	60,924.22
1990 total	104,352.22	388,159.89	208,448.44	16,965.18	14,223.99	62,458.33	794,608.06

Between 2000 and 2010 (Table 4), there was 1671.11 km^2 water area transferred to other land cover types, accounting for 12.17% of the area of water area in 2000. There was 6627.46 km^2 desert or other land transferred to other land cover types, accounting for

10.88% of the area of desert or other land in 1990. Additionally, there was 19,036.32 km^2 cropland transferred to other land cover types, accounting for 9.02% of the area of cropland in 2000. The transformed area of built-up land is less than that of other land cover types, which was only 1400.09 km^2. Among them, 67.42% of the desert or other land was transformed to grassland, and 59.64% of the built-up land was converted to cropland.

Table 4. Transformed areas of each land cover type in YRB between 2000 and 2010 (unit: km^2).

2010 \ 2000	Forest	Grassland	Cropland	Built-Up Land	Water Area	Desert or Other Land	2010 Total
Forest	101,801.05	2379.16	2545.18	55.00	60.00	455.03	107,295.42
Grassland	923.06	370,760.69	7520.52	354.02	355.02	4468.31	384,381.62
Cropland	628.04	4374.30	192,001.30	835.06	650.05	584.04	199,072.79
Built-up land	453.03	2972.21	6985.48	17,029.18	201.01	691.05	28,331.96
Water area	108.01	655.05	1025.07	48.00	12,065.84	429.03	14,331.00
Desert or other land	134.01	5291.37	960.07	108.01	405.03	54,296.76	61,195.25
2000 total	104,047.20	386,432.78	211,037.62	18,429.27	13,736.95	60,924.22	794,608.06

Between 2010 and 2020 (Table 5), there was 602.04 km^2 water area transferred to other land cover types, accounting for 4.27% of the area of water area in 2010. There was 6178.43 km^2 cropland transferred to other land cover types, accounting for 3.05% of the area of cropland in 2010. The transformed area of built-up land is less than that of other land cover types, which was only 400.02 km^2. Among them, 85.00% of the built-up land was transformed to cropland, and 67.43% of the cropland was converted to built-up land.

Table 5. Transformed areas of each land cover type in YRB between 2010 and 2020 (unit: km^2).

2020 \ 2010	Forest	Grassland	Cropland	Built-Up Land	Water Area	Desert or Other Land	2020 Total
Forest	105,911.34	546.04	539.04	10.00	22.00	267.02	107,295.44
Grassland	635.04	381,758.45	1036.07	25.00	131.01	796.06	384,381.63
Cropland	393.03	1466.10	196,359.61	340.02	221.02	293.02	199,072.80
Built-up land	348.02	2250.16	4166.29	20,779.44	156.01	632.04	28,331.96
Water area	69.00	248.02	388.03	25.00	13,481.93	119.01	14,330.99
Desert or other land	30.00	255.02	49.00	0.00	72.00	60,789.21	61,195.23
2010 total	107,386.43	386,523.79	202,538.04	21,179.46	14,083.97	62,896.36	794,608.06

The mutual converted types of land cover were mainly occurred between cropland, grassland, forest, desert, or other land during the three periods from 1990 to 2000, 2000 to 2010, and 2010 to 2020, while most of the increased built-up land was mainly transformed from cropland.

3.5. Drivcing Forces of Land Cover Change

3.5.1. Single Factor Analysis

In this study, the change of land cover type is taken as the dependent variables, and the elevation, precipitation, temperature, NDVI, population density, and GDP were taken as the independent variables.

According to the factor detector, the influence of each factor on the land cover change in the YRB was revealed, and the q value of each driving factor was not very high. The detected results were list in Table 6. Take 2020 as an example. The order of explanatory power of land cover drivers was population density > elevation > temperature > precipitation > GDP > NDVI. The population density is the first dominant factor affecting the land cover change in the YRB area, which average contribution rate is up to 0.264; the second dominant factor is elevation, with an average contribution rate of 0.234. So, human activities, such as regional urbanization processes, as reflected by population density, are the most important economic and social factors affecting land cover change, and the explanatory power of elevation and temperature factors on land cover exceeds 20%, which is the natural factor that causes the main impact, while the explanatory influence of individual factors, such as average annual precipitation, NDVI, and GDP, is relatively small.

Table 6. The q value of each detection factor varies to land cover change from 1990 to 2020.

	Elevation	Precipitation	Temperature	NDVI	Population Density	GDP
1990	0.229	0.111	0.226	0.123	0.245	0.139
2000	0.245	0.111	0.241	0.109	0.283	0.138
2010	0.223	0.06	0.227	0.131	0.284	0.125
2020	0.239	0.129	0.221	0.097	0.245	0.126
Average	0.234	0.103	0.229	0.115	0.264	0.132

3.5.2. Detection of Factor Interactions

The interaction detector assesses whether the explanatory powers of two factors are enhanced, weakened, or independent of each other. First, the q values of two factors X_1 and X_2 for Y were calculated ($q(X_1)$ and $q(X_2)$). Then, the q value of interaction was calculated ($q(X_1 \cap X_2)$) and compared with $q(X_1)$ and $q(X_2)$ to indicate the interaction type between two variables.

Taking the 2010 results as an example (the results of 1990, 2000, and 2020 are the same as their mode of action), green represents bilinear enhancement of two factors, i.e., $q(X_1 \cap X_2) > \text{Max}\ (q(X_1), q(X_2))$, yellow represents nonlinear enhancement of two factors, i.e., $q(X_1 \cap X_2) > (q(X_1) + q(X_2))$, and unfilled numbers represent the force of single factor action. It can be seen from the interaction detection results (Table 7), the interaction of each factor shows a nonlinear enhancement and two-factor enhancement, and the overall performance is that the interaction of each factor is enhanced, indicating that there is significant coordination and correlation between the factors. Combining the results of single-factor detection and multi-factor interaction detection, we can see that the q value of any two driving factors on the spatial distribution of land cover is higher than that of a single driving factor.

Table 7. The explanatory power of factor interactions.

	Elevation	Precipitation	Temperature	NDVI	Population Density	GDP
Elevation	0.244					
Precipitation	0.375	0.114				
Temperature	0.292	0.352	0.242			
NDVI	0.374	0.24	0.365	0.109		
Population density	0.344	0.329	0.331	0.33	0.283	
GDP	0.267	0.243	0.264	0.235	0.289	0.138

The six groups of interaction factors with strong explanatory power for land cover change were elevation ∩ precipitation > elevation ∩ NDVI > temperature ∩ NDVI > precipitation ∩ temperature > elevation ∩ population density > population density ∩ temperature. The multi-factor interaction analyzed results show that land cover change in YRB was most driven by the interaction between elevation and precipitation, and the second influence on land cover change was the interaction between elevation and NDVI in YRB area from 1990 to 2020, which indicates the joint driving influence of natural factors and human factors could be better to express the explanatory power of the distribution change of land cover.

3.5.3. Significant Differences between Factors

Taking 2010 as an example (Table 8), we use the ecological detector to judge whether the effects of the two factors on land cover changes are significantly different at a confidence level of 0.95. Y represents that there is a significant difference in the effects of the two factors on land cover changes, and N represents no significant difference.

Table 8. Significant differences between driving factors of land cover change.

	Elevation	Precipitation	Temperature	NDVI	Population Density	GDP
Elevation						
Precipitation	Y					
Temperature	N	Y				
NDVI	Y	Y	Y			
Population density	Y	Y	Y	Y		
GDP	Y	N	Y	N	Y	

Except for temperature and elevation, GDP and precipitation, and GDP and NDVI, most factors have significantly different effects on land cover change (Table 8). We found that the factor population density, which had greater contributions, all had statistically significant differences with other factors. In addition, elevation and temperature are also basically statistically different from other factors. Therefore, population density is the most critical factor affecting land cover change in the YRB area, followed by factors such as elevation and temperature.

Through single-factor detection analyzations, the land cover change in the YRB area was significantly driven by the factors of population density, elevation, and temperature. The multi-factor interaction detection analysis shows that the influence degree of any two driving factors interaction was greater than that of a single factor (Tables 6 and 7). Moreover, the statistical test analysis of the ecological detector indicates that the population density, elevation, and temperature show the statistically significantly difference from other factors. The single factor detection and factor interaction detection show that the larger the q value of a single factor, the larger the q value of the corresponding factor interaction [36]. Therefore, it can be speculated that the change of land cover was driven by multiple factors.

4. Discussion

Since the 1990s, large-scale reclamation in the YRB area has led to a series of ecological and environmental problems, such as soil erosion, local ecosystem degradation, and reduced water conservation functions [37]. The study of land cover change in the YRB is an important basis for the rational development and utilization of land resources and ecological restoration in the YRB area. Based on the land cover data of the YRB in 1990, 2000, 2010, and 2020, this study introduced a land cover dynamic index model and a land cover transition matrix to quantitatively analyze the dynamic changes of land cover and explicate the change trend of land cover in the YRB area since 1990. The results show that grasslands, forests, and croplands are the three major land cover types in the YRB area, and their area covered about 85% of the whole area, in which the area of grassland is the largest. In general, the dominated land cover type in UA, MA, and DA were grasslands, croplands, and croplands, respectively.

In recent years, Chinese government has paid more and more attention to improving the ecological environment, especially in the YRB area. The implementation of ecological protection policies (such as GGP program) was the leading driving force for the conversion of cropland to forest and grassland in China. Due to rebuilding a graceful northwest with green mountains and clean water, a national arable land reserve program (called the GGP) of China was released in 1999. The GGP program is considered one of the largest conservation projects in the world [38], in which the cropland with a slope more than 25° were transformed to woodland and grassland. By analyzing the changes in land cover from 1990 to 2020, we found the area of forest and grassland has been increasing since 2000, while the area of cropland has decreased; there were many transfers between croplands, forests, and grasslands, which indicates that the policy has played an important role in the YRB area and has greatly promoted the improvement of the ecological environment and the sustainable development of the region.

With the acceleration of China's industrialization and urbanization, the distribution of land cover has undergone a series of changes. Built-up land has continued to increase, from less than 2.14% in 1990 up to 3.57% in 2020, even occupying some cropland. For this reason, the Chinese government has formulated a series of land cover policies to deal with these problems and challenges, including "requisition-compensation balance of arable land" and "increasing vs. decreasing balance of urban-rural built land" [39], which are aimed at reducing cropland occupied by built-up land and protecting cropland. Through the implementation of these policies, part of the rural built-up land has been reclaimed into cropland, which has promoted the conversion of built-up land and unused land into cropland. However, the implementation of these policies has not effectively slowed down the rate of urban expansion taking up cropland. Our research results show that there was 4166.29 km^2 of cropland converted to built-up land, accounting for 55.16% of the total area converted to built-up land during the period from 2010 to 2020. Obviously, the implementation of land management policies has not effectively prevented the expansion of built-up land. While urban expansion occupies cropland, China has also emphasized the replenishment of cropland through the integration of vacant residential land, industrial and mining land, and other land cover types.

Land cover change is influenced by the interaction of multiple drivers. This paper explicitly analyzes the driving forces of social and natural factors on land cover changes, based on GeoDetector. Through single-factor detection, the dominant factor of land cover change was population density, with an average contribution rate of 0.264. Additionally, the population growth has long been considered a major factor leading to land cover changes [40]. The detection of significant differences between the driving factors by the ecological detector shows that there were statistically significant differences between population density and other factors. The second most dominant factor in the spatial distribution of land cover is elevation. As altitude increases, NDVI decreases, and human activity decreases, resulting in spatial differences in land cover. In addition, the analysis of single factor driving also conducts further research on the spatial distribution of land cover from the aspect of multi-factor interaction. From the multi-factor interaction test results, it can be concluded that land cover change is most driven by the interaction between elevation and precipitation; the second influence on land cover change is the interaction between elevation and NDVI. Through the joint driving influence of natural factors and human factors, the explanatory power of the spatial distribution of land cover is stronger.

The spatial distribution of land cover was influenced by many driving factors including nature, society, and human [22,41,42]. Thus, it should be pay more attention to focus on understating the impact of human activities on land cover change, especially in the ecologically fragile areas of YRB, which is an important basis for promoting social economic development and maintaining the balance tween human needs and ecological environment health. Moreover, policy influence on land cover change should be considered in the future work.

5. Conclusions

Based on the land cover data of the YRB in 1990, 2000, 2010, and 2020, the methods of dynamic degree index, transfer matrix, and GeoDetector were introduced to explicate the spatiotemporal change of land cover and analyze their driving forces in the YRB area. The results show that, from 1990 to 2020, the grassland, cropland, and forest were the major land cover type in the YRB area. The dominated type of land cover in UA, MA, and DA were grassland, cropland, and cropland, respectively. The area of forest and grassland showed an increasing trend, area of cropland showed a continual decreasing trend, and area of built-up land showed a continual increased trend science 2000. Mutual conversions between cropland, grassland, forest, desert, or other land were the transform patterns of land cover change in the YRB area during the period from 1990 to 2020. Most of the built-up land was transferred from cropland, especially in the period from 2010 to 2020. In addition, the analyzed of driving factors on land cover change indicates that population density was the key influence factor, followed by the impact of elevation and temperature on land cover change in the YRB area during the period from 1990 to 2020.

Author Contributions: Conceptualization, Z.F.; Data curation, Z.F. and S.Z.; Formal analysis, Z.F., S.Z. and X.G.; Investigation, S.Z. and Z.F.; Methodology, Z.F. and S.Z.; Resources, Z.F. and S.Z.; Software, Z.F. and S.Z.; Supervision, Z.F. and X.G.; Validation, S.Z. and Z.F.; Visualization, S.Z. and Z.F.; Writing—original draft, S.Z. and Z.F.; Writing—review & editing, Z.F. and S.Z.; Project administration, Z.F.; Funding acquisition, Z.F. All authors have read and agreed to the published version of the manuscript.

Funding: This research was funded by the National Natural Science Foundation of China, grant number (41971358, 41930647 and 41931293); National Key R&D Program of China, grant number (2017YFA0603702); and the Innovation Project of State Key Laboratory of Re-sources and Environmental Information System, grant number (O88RA600YA).

Institutional Review Board Statement: Not applicable.

Informed Consent Statement: Not applicable.

Data Availability Statement: The land cover data, DEM, precipitation, temperature, population density, and GDP data are available from http://www.resdc.cn. All relevant data generated during the study are available from the corresponding author upon reasonable request.

Conflicts of Interest: The authors declare no conflict of interest.

References

1. Liu, J.; Kuang, W.; Zhang, Z.; Xu, X.; Qin, Y.; Ning, J.; Zhou, W.; Zhang, S.; Li, R.; Yan, C.; et al. Spatiotemporal characteristics, patterns, and causes of land-use changes in China since the late 1980s. *J. Geogr. Sci.* **2014**, *24*, 195–210. [CrossRef]
2. Moran, E.; Ojima, D.S.; Buchmann, B.; Canadell, J.G.; Coomes, O.; Graumlich, L.; Jackson, R.; Jaramillo, V.; Lavorel, S.; Leadley, P.J. Global Land Project: Science plan and implementation strategy. *Environ. Policy* **2005**. Available online: https://publications.csiro.au/rpr/pub?list=BRO&pid=procite:b734a29e-14aa-4a06-8527-beef55ff7a39 (accessed on 10 March 2021).
3. Li, X.; Fang, J.; Piao, S.J. Landuse changes and its implication to the ecological consequences in Lower Yangtze Region. *Acta Geograph. Sin.* **2003**, *58*, 659–667.
4. Turner, B.L.I.; Skole, D.L.; Sanderson, S.; Fischer, G.; Fresco, L.; Leemans, R.J. Land-Use and Land-Cover Change. Science/Research Plan. Global Change Report 1995. Available online: https://pure.iiasa.ac.at/id/eprint/4402/ (accessed on 10 March 2021).
5. Zhang, Z.; Wang, X.; Wen, Q.; Zhao, X.; Liu, F.; Zuo, L.; Shunguang, H.U.; Jinyong, X.U.; Ling, Y.I.; Liu, B.J. Research progress of remote sensing application in land resources. *J. Remote Sens.* **2016**, *20*, 1243–1258.
6. Zhang, Y.; Lu, X.; Liu, B.; Wu, D.; Fu, G.; Zhao, Y.; Sun, P. Spatial relationships between ecosystem services and socioecological drivers across a large-scale region: A case study in the Yellow River Basin. *Sci. Total Environ.* **2020**, *766*, 142480. [CrossRef] [PubMed]
7. Ji, Q.; Liang, W.; Fu, B.; Zhang, W.; Yan, J.; Lü, Y.; Yue, C.; Jin, Z.; Lan, Z.; Li, S.; et al. Mapping Land Use/Cover Dynamics of the Yellow River Basin from 1986 to 2018 Supported by Google Earth Engine. *Remote Sens.* **2021**, *13*, 1299. [CrossRef]
8. Lambin, E.F.; Meyfroidt, P. Land use transitions: Socio-ecological feedback versus socio-economic change. *Land Use Policy* **2010**, *27*, 108–118. [CrossRef]
9. Rimal, B.; Baral, H.; Stork, N.E.; Paudyal, K.; Rijal, S. Growing City and Rapid Land Use Transition: Assessing Multiple Hazards and Risks in the Pokhara Valley, Nepal. *Land* **2015**, *4*, 957–978. [CrossRef]
10. Bik, I.; Jeleek, L.; Štěpánek, V. Land-Use Changes and their Social Driving Forces in Czechia in the 19th and 20th Centuries. *Land Use Policy* **2001**, *18*, 65–73.
11. Fu, B.; Wang, S.; Liu, Y.; Liu, J.; Liang, W.; Miao, C. Hydrogeomorphic Ecosystem Responses to Natural and Anthropogenic Changes in the Loess Plateau of China. *Annu. Rev. Earth Planet. Sci.* **2017**, *45*, 223–243. [CrossRef]
12. Yongge, L.; Wei, L.; Qi, F.; Meng, Z.; Linshan, Y.; Jutao, Z. Effects of land use and land cover change on soil organic carbon storage in the Hexi regions, Northwest China. *J. Environ. Manag.* **2022**, *312*, 114911.
13. Surya, B.; Ahmad, D.N.A.; Sakti, H.H.; Sahban, H. Land Use Change, Spatial Interaction, and Sustainable Development in the Metropolitan Urban Areas, South Sulawesi Province, Indonesia. *Land* **2020**, *9*, 95. [CrossRef]
14. Teklay, A.; Dile, Y.T.; Setegn, S.G.; Demissie, S.S.; Asfaw, D.H. Evaluation of static and dynamic land use data for watershed hydrologic process simulation: A case study in Gummara watershed, Ethiopia. *Catena* **2018**, *172*, 65–75. [CrossRef]
15. Dewan, A.M.; Yamaguchi, Y. Land use and land cover change in Greater Dhaka, Bangladesh: Using remote sensing to promote sustainable urbanization. *Appl. Geogr.* **2009**, *29*, 390–401. [CrossRef]
16. Kalnay, E.; Cai, M. Impact of urbanization and land-use change on climate. *Nature* **2003**, *423*, 528. [CrossRef] [PubMed]
17. Liu, Q.; Yang, D.; Cao, L.; Anderson, B. Assessment and Prediction of Carbon Storage Based on Land Use/Land Cover Dynamics in the Tropics: A Case Study of Hainan Island, China. *Land* **2022**, *11*, 244. [CrossRef]
18. Tba, B.; Dama, C.J. Land use and land cover dynamics and drivers in the Muga watershed, Upper Blue Nile basin, Ethiopia. *Remote Sens. Appl. Soc. Environ.* **2019**, *15*, 100249.

19. Li, K.; Feng, M.; Biswas, A.; Su, H.; Niu, Y.; Cao, J. Driving Factors and Future Prediction of Land Use and Cover Change Based on Satellite Remote Sensing Data by the LCM Model: A Case Study from Gansu Province, China. *Sensors* **2020**, *20*, 2757. [CrossRef]
20. Bekele, B.; Wu, W.; Yirsaw, E. Drivers of Land Use-Land Cover Changes in the Central Rift Valley of Ethiopia. *Sains Malays.* **2019**, *48*, 1333–1345. [CrossRef]
21. Mlba, B.; At, C.; Nh, D.; Dtm, E.; Ea, E.; Mt, C.; Tm, F.; Aaf, C.; Ds, B.; Mya, B.J. Exploring land use/land cover changes, drivers and their implications in contrasting agro-ecological environments of Ethiopia. *Land Use Policy* **2019**, *87*, 104052.
22. Cui, J.; Zhu, M.; Liang, Y.; Qin, G.; Li, J.; Liu, Y. Land Use/Land Cover Change and Their Driving Factors in the Yellow River Basin of Shandong Province Based on Google Earth Engine from 2000 to 2020. *ISPRS Int. J. Geo-Inf.* **2022**, *11*, 163. [CrossRef]
23. Fan, H.; Chen, S.; Li, Z.; Liu, P.; Xu, C.; Yang, X. Assessment of heavy metals in water, sediment and shellfish organisms in typical areas of the Yangtze River Estuary, China. *Mar. Pollut. Bull.* **2020**, *151*, 110864. [CrossRef] [PubMed]
24. Wang, J.; Xu, C.J. Geodetector: Principle and prospective. *Acta Geogr. Sin.* **2017**, *72*, 116–134.
25. Han, J.; Wang, J.; Chen, L.; Xiang, J.; Ling, Z.; Li, Q.; Wang, E. Driving factors of desertification in Qaidam Basin, China: An 18-year analysis using the geographic detector model. *Ecol. Indic.* **2021**, *124*, 107404. [CrossRef]
26. Nie, T.; Dong, G.; Jiang, X.; Lei, Y. Spatio-Temporal Changes and Driving Forces of Vegetation Coverage on the Loess Plateau of Northern Shaanxi. *Remote Sens.* **2021**, *13*, 613. [CrossRef]
27. Peng, W.; Kuang, T.; Tao, S. Quantifying influences of natural factors on vegetation NDVI changes based on geographical detector in Sichuan, western China. *J. Clean. Prod.* **2019**, *233*, 353–367. [CrossRef]
28. Zhang, J.; Yu, L.; Li, X.; Zhang, C.; Shi, T.; Wu, X.; Yang, C.; Gao, W.; Li, Q.; Wu, G. Exploring Annual Urban Expansions in the Guangdong-Hong Kong-Macau Greater Bay Area: Spatiotemporal Features and Driving Factors in 1986–2017. *Remote Sens.* **2020**, *12*, 2615. [CrossRef]
29. Jiang, W.; Yuan, L.; Wang, W.; Cao, R.; Zhang, Y.; Shen, W. Spatio-temporal analysis of vegetation variation in the Yellow River Basin. *Ecol. Indic.* **2014**, *51*, 117–126. [CrossRef]
30. Liu, J.; Zhang, Z.; Zhuang, D. Study on the Spatial-Temporal Dynamic Change of Land-use Change and Diving Forces Analyses in1990s. *Bull. Chin. Acad. Sci.* **2003**, *1*, 1–12.
31. Liu, J.; Zhang, Z.; Xu, X.; Kuang, W.; Zhou, W.; Zhang, S.; Li, R.; Yan, C.; Yu, D.; Jiang, N. Spatial patterns and driving forces of land use change in China during the early 21st century. *J. Geogr. Sci.* **2010**, *20*, 483–494. [CrossRef]
32. Ning, J.; Liu, J.; Kuang, W.; Xu, X.; Zhang, S.; Yan, C.; Li, R.; Wu, S.; Hu, Y.; Du, G.; et al. Spatiotemporal patterns and characteristics of land-use change in China during 2010–2015. *J. Geogr. Sci.* **2018**, *28*, 547–562. [CrossRef]
33. Zhou, Y.; Li, X.; Liu, Y. Land use change and driving factors in rural China during the period 1995–2015. *Land Use Policy* **2020**, *99*, 105048. [CrossRef]
34. Pontius, R.G.; Huang, J.; Jiang, W.; Khallaghi, S.; Lin, Y.; Liu, J.; Quan, B.; Ye, S. Rules to write mathematics to clarify metrics such as the land use dynamic degrees. *Landsc. Ecol.* **2017**, *32*, 2249–2260. [CrossRef]
35. Chen, M.; Bai, Z.; Wang, Q.; Shi, Z. Habitat Quality Effect and Driving Mechanism of Land Use Transitions: A Case Study of Henan Water Source Area of the Middle Route of the South-to-North Water Transfer Project. *Land* **2021**, *10*, 796. [CrossRef]
36. Zhang, X.; Lyu, C.; Fan, X.; Bi, R.; Xia, L.; Xu, C.; Sun, B.; Li, T.; Jiang, C. Spatiotemporal Variation and Influence Factors of Habitat Quality in Loess Hilly and Gully Area of Yellow River Basin: A Case Study of Liulin County, China. *Land* **2022**, *11*, 127. [CrossRef]
37. Liu, Y.; Yang, Y.; Li, Y.; Li, J. Conversion from rural settlements and arable land under rapid urbanization in Beijing during 1985–2010. *J. Rural Stud.* **2017**, *51*, 141–150. [CrossRef]
38. Wang, S.-Y.; Liu, J.-S.; Ma, T.-B. Dynamics and changes in spatial patterns of land use in Yellow River Basin, China. *Land Use Policy* **2010**, *27*, 313–323. [CrossRef]
39. Liu, Y.; Fang, F.; Li, Y. Key issues of land use in China and implications for policy making. *Land Use Policy* **2014**, *40*, 6–12. [CrossRef]
40. Lin, G.C.; Ho, S.P. China's land resources and land-use change: Insights from the 1996 land survey. *Land Use Policy* **2003**, *20*, 87–107. [CrossRef]
41. Zhou, X.; Zhou, Y. Spatio-Temporal Variation and Driving Forces of Land-Use Change from 1980 to 2020 in Loess Plateau of Northern Shaanxi, China. *Land* **2021**, *10*, 982. [CrossRef]
42. Vu, T.-T.; Shen, Y. Land-Use and Land-Cover Changes in Dong Trieu District, Vietnam, during Past Two Decades and Their Driving Forces. *Land* **2021**, *10*, 798. [CrossRef]